

State Space Models on Temporal Graphs: A First-Principles Study

Jintang Li^{1*}, Ruofan Wu^{2*}, Xinzhou Jin¹, Boqun Ma³, Liang Chen¹, Zibin Zheng¹

¹Sun Yat-sen University, ²Fudan University, ³Shanghai jiao tong University

✉ Primary contact: lijt55@mail2.sysu.edu.cn

Abstract

Over the past few years, research on deep graph learning has shifted from static graphs to temporal graphs in response to real-world complex systems that exhibit dynamic behaviors. In practice, temporal graphs are formalized as an ordered sequence of static graph snapshots observed at discrete time points. Sequence models such as RNNs or Transformers have long been the predominant backbone networks for modeling such temporal graphs. Yet, despite the promising results, RNNs struggle with long-range dependencies, while transformers are burdened by quadratic computational complexity. Recently, state space models (SSMs), which are framed as discretized representations of an underlying continuous-time linear dynamical system, have garnered substantial attention and achieved breakthrough advancements in *independent* sequence modeling. In this work, we undertake a principled investigation that extends SSM theory to temporal graphs by integrating structural information into the online approximation objective via the adoption of a Laplacian regularization term. The emergent continuous-time system introduces novel algorithmic challenges, thereby necessitating our development of GRAPHSSM, a graph state space model for modeling the dynamics of temporal graphs. Extensive experimental results demonstrate the effectiveness of our GRAPHSSM framework across various temporal graph benchmarks.

1 Introduction

As a class of neural networks designed to operate directly on graph-structured data, graph neural networks (GNNs) [22, 41] have achieved remarkable success and have established new state-of-the-art performance across a broad spectrum of graph-based learning tasks [19]. While significant progress has been made in researching *static* graphs, many real-world networks, such as social, traffic, and financial networks may exhibit *temporal* behaviors that carry valuable time information [20]. This gives rise to temporal (dynamic) graphs, wherein the nodes and edges of the graph may undergo constant or periodic changes over time. In applications where temporal graphs arise, modeling and exploiting the dynamic nature of the continuously evolving graph is crucial in representing the underlying data and achieving high predictive performance [23, 42].

Learning over temporal graphs is typically approached as a sequence modeling problem in which graph snapshots form a sequence [33]. This often involves challenges related to long graph sequences and scalability issues [24]. Recurrent neural networks (RNNs) [44, 4, 18] have historically dominated sequence modeling over the last years. However, they have long been plagued by the poor capability in modeling long sequences in terms of rapid forgetting. This hampers their performance in temporal graphs that require a broader context or longer time window to capture relevant dependencies and patterns. Recently, the advancement of Transformers [40] has led to a shift in this paradigm, given

*Equal contribution.

their superior performance. Yet, Transformers also struggle with long sequence learning due to the computational and memory complexity of self-attention is quadratically dependent on the sequence length. The overwhelming computation and memory requirements/cost associated with Transformers makes them less applicable in practical application handling long-term sequences [49].

Recently, state space models (SSMs) have emerged as a powerful tool for sequence modeling [11, 13, 28, 39, 6, 10]. The salient characteristic that distinguishes state space models as particularly compelling is their conceptualization of sequential inputs as discrete observations from an underlying process evolving in continuous time, which naturally arises in scenarios such as speech processing [39] and time series analysis [47]. SSMs sustain a latent state throughout an input sequence and formulate state update equations through the discretization of an underlying linear dynamical system (LDS). Owing to their invariant state size, SSMs exhibit an efficient inferential time complexity, akin to that of RNNs. Simultaneously, they overcome the long-range modeling deficiencies inherent to RNNs through meticulous initializations of state matrices which are theoretically shown to achieve an optimal compression of history [11].

Temporal graphs often manifest as discrete snapshots capturing the evolution of an underlying graph that is inherently dynamic and continuous in nature [21]. In this context, the SSM methodology could be appropriated as a foundational primitive for temporal graph modeling. However, SSMs are predominantly architected towards independent sequence modeling. Hence, the task of systematically incorporating time-varying structural information into the SSM framework poses significant challenge. Specifically, it remains unexplored as to whether the foundational methodology of discretized LDS is readily applicable to the domain of temporal graphs.

In this work, we advance the SSM methodology to encompass temporal graphs from first principles. Rather than presupposing the evolution of the underlying temporal graph, we penetrate into the fundamental problem of online function approximation that underpins the theoretical development of SSMs for sequence modeling [11]. By solving a novel Laplacian regularized online approximation objective, we derive a piecewise dynamical system that compresses historical information of temporal graphs. The piecewise nature of the obtained continuous-time system poses new challenges toward discretization into linear recurrences, thereby motivates our design of GRAPHSSM, a state space framework for temporal graphs. The main contributions of this work are summarized as follows:

- We introduce the GHIPPO abstraction, a novel construct predicated on the objective of Laplacian regularized online function approximation. This abstraction can be alternatively conceptualized as a memory compression primitive that simultaneously compresses both feature the dynamics alongside the evolving topological structure of the underlying temporal graph. The solution to GHIPPO is characterized by a dynamical system that is piecewise linear in node feature inputs.
- We introduce GRAPHSSM, a flexible state space framework designed for temporal graphs, which effectively addresses the key algorithmic challenge of unobserved graph mutations that impedes the straightforward discretization of the GHIPPO solution into (linear) recurrences through employing a novel mixed discretization strategy.
- Experimental results on six temporal graphs have validated the effectiveness of GRAPHSSM. In particular, GRAPHSSM has the advantages in scaling efficiency compared to existing state-of-the-arts, which can generalize to temporal graphs with long-range snapshots.

2 Related work

2.1 Temporal graph learning

A major branch of temporal graph learning methods consists of snapshot-based methods, which handle discrete-time temporal graphs by learning the temporal dependencies across a sequence of time-stamped graphs. Snapshot-based methods have been extensively studied in the literature due to their flexibility in modeling temporal graphs and ease of implementation [24]. Early works mainly focus on learning node representations by simulating temporal random walks [38] or modeling the triadic closure process [48] on multiple graph snapshots. These methods typically generate piecewise constant representations and may suffer from the staleness problem [20]. In recent years, the most established solution has been switched to combine sequence models (e.g., RNNs [44] and SNNs [37, 8]) with static GNNs to capture temporal dependencies and correlations between snapshots [45, 33, 38, 24]. To better translate the success achieved on static graphs in both their

design and training strategies, recent frameworks such as ROLAND [46] and its variants [51, 17] have been proposed to repurpose static GNNs to temporal graphs. There is another important line of research that focuses on continuous-time temporal graphs, we kindly refer readers to [26] and [20] for comprehensive surveys on this research topic.

2.2 State Space Models

State space models (SSMs) have historically served as a pivotal tool in fields such as signal processing [29] and time series analysis [3]. In recent advancements, they have also seen active adoption as a layer within neural sequence modeling frameworks [11, 13, 28, 39, 10]. The linear nature of SSMs confers several significant advantages. Key among these is the better-controlled stability that enables effective long range modeling through careful initializations of state space layer parameters [11, 30], with the most representative method being HiPPO [11], a theory-driven framework notable for its optimal memory compression on continuous sequence inputs. Moreover, the computational efficacy of SSMs is notably enhanced through the use of techniques such as convolutions [13, 6] or parallel scans [39]. The promising properties of SSMs also attracts further explorations on graphs [2].

Comparison. The usual paradigms for designing sequence models over graphs involve recurrence (e.g. RNNs [44]), integrate-and-fire (e.g. SNNs [37, 8]), or attention (e.g. Transformers [40]), which each come with tradeoffs [14]. For example, RNNs are a natural recurrence model for sequential modeling that require only constant computation/storage per time step, but are slow to train and suffer from the rapid forgetting issue. This empirically limits their ability to handle long sequences. SNNs share a similar recurrent architecture with RNNs while using 1-bit spikes to transmit temporal information, which would sacrifice expressivity and potentially suffer from optimization difficulties (e.g., the “vanishing gradient problem”) [25]. Transformers encode local context via attention mechanism and enjoy fast, parallelizable training, but are not sequential, resulting in more expensive inference and an inherent limitation on the context length. Compared to the aforementioned architectures, SSMs particularly the promising Mamba (S6) model [10], offer advantages such as fast training and inference, along with fewer parameters and comparable performance. These characteristics make SSMs particularly well-suited for sequence modeling, even (or especially) on extremely long sequences. Comparison among these architectures are illustrated in Table 1

Table 1: Comparison of different neural network architectures for sequence modeling.

	RNNs [44, 4, 18]	SNNs [37, 8]	Transformers [40]	SSMs (S6 [10])
Training	Slow	Slow	Fast	Fast
Inference	Fast	Fast	Slow	Fast
Para. Size	Medium	Extremely small	Large	Small
Performance	☆☆☆	☆☆☆	☆☆☆☆☆	☆☆☆☆☆
Limitations	Forgetting	Vanishing gradients	Mem. & Time: $O(n^2)$?

3 The GRAPHSSM framework

The primary motivation of our framework is the fact that discrete-time temporal graphs are sequential observations of an underlying temporal graph that evolves continuously. Adopting this functional viewpoint, we will first develop a piecewise recurrent memory update scheme in section 3.1 that optimally approximates the underlying continuous-time temporal graph, utilizing a novel extension of the HiPPO abstraction to graph-typed inputs [11]. The proposed framework retains many nice properties of HiPPO while posing the new challenge of *unobserved graph mutation* when handling discretely-observed observations, which we analyze in section 3.2 and propose a mixing mechanism to improve the recurrent approximation. Finally, we present our GRAPHSSM framework in section 3.3. Overview of GRAPHSSM is shown in Figure 1.



Figure 1: GRAPHSSM framework.

3.1 GHIPPO: HIPPO on temporal graphs

Setup We fix a time interval $[0, T]$. A temporal graph on $[0, T]$ is characterized by two *processes* G and X : For each $t \in [0, T]$, the process G maps t to a graph object $G(t) = (V(t), E(t))$. We assume the node process $V(t)$ to be fixed over time, i.e., $V(t) \equiv V, t \in [0, T]$ with $N_V = |V|$ and discuss the case for varying node processes in appendix B.2. The edge process $E(t)$ is a piecewise-constant process with a finite number M of mutations over $[0, T]$ that are described via a sequence of *events*:

$$\mathcal{E} = \{\mathcal{E}_1, \dots, \mathcal{E}_M\} \text{ with each } \mathcal{E}_m = (u_m, v_m, t_m, a_m), 1 \leq m \leq M. \quad (1)$$

Each event \mathcal{E}_m constitutes an interaction between node pair (u_m, v_m) at time t_m with action a_m , the action could be either insertion or deletion. The evolution process is thus depicted as the following:

$$G(0) \xrightarrow{\mathcal{E}_1} G(t_1) \xrightarrow{\mathcal{E}_2} G(t_2) \longrightarrow \dots \longrightarrow G(t_{M-1}) \xrightarrow{\mathcal{E}_M} G(t_M) = G(T). \quad (2)$$

The process X maps t to a node feature matrix $X(t) \in \mathbb{R}^{N_V \times d}$ with feature dimension d . Throughout this paper it is often helpful to view G and X as graph-valued and matrix-valued *functions*. In typical discrete-time temporal graph learning problems, the underlying graph is observed at timestamps τ_1, \dots, τ_L with time gaps $\Delta_l = \tau_l - \tau_{l-1}, 2 \leq l \leq L$. The observations thus form a sequence of snapshots $\{G(\tau_l), X(\tau_l)\}_{1 \leq l \leq L}$ which are abbreviated as $\{G_{1:L}, X_{1:L}\}$. Notably, the observation times are usually *interleaved with* the mutation times, resulting in the majority of mutation times remain unobserved. This situation presents significant challenges in effective modeling the dynamics of graph evolution, a topic that will be further explored subsequently.

The HIPPO abstraction algorithmically, the goal of continuous-time dynamic modeling is to design a *memory module* that optimally compresses all the historical information[11]. Under the context of univariate sequence modeling, the HIPPO framework [11] formalizes the memory compression problem into an online approximation problem in some function space and derive HIPPO operators under specific types of basis functions, among which the HIPPO-LEGS configuration has become the state-of-the-art in state-space sequence modeling paradigms [13, 39]. However, naively extending HIPPO abstraction to graph learning scenarios (via treating node features as inputs) could be deemed inadequate since HIPPO handles distinct inputs *independently*, without the capability to incorporate the interconnectivity information among various inputs which could potentially enhance the efficiency of memory compression. For illustrative purposes, in instances where input observations are noisy, the exploitation of neighborhood information has the potential to facilitate a denoising step, as evidenced in image processing applications [32] and semi-supervised learning primitives [50, 43]. To systematically utilize the connectivity information, we propose a new approximation paradigm, the *Laplacian-regularized online approximation* that extends HIPPO to graph modeling frameworks. Formally, we start with the simple setup with $d = 1$, i.e., each node possesses a scalar feature, and we propose an approximation scheme that simultaneously approximates the history of all the N_V inputs up until time t , i.e., $\{X(s), s \in [0, t]\}$ using their corresponding memories at time t , i.e., $Z(t) = \{z_v(t)\}_{v \in V} \in \mathbb{R}^{N_V \times 1}$ according to the following objective at time t :

$$\mathcal{L}_t(Z; G, X, \mu) = \int_0^t \|X(s) - Z(s)\|_2^2 d\mu_t(s) + \alpha \int_0^t Z(s)^\top L(s) Z(s) d\mu_t s. \quad (3)$$

Here $\alpha > 0$ is a balancing constant, μ_t is a time-dependent measure that is supported on the interval $[0, t]$ which controls the importance of various parts of the input domain² and $L(t)$ is a normalized Laplacian at time t , which allows definition such as the symmetric normalized Laplacian $L_{\text{sym}}(s) = I - D(s)^{-1/2} A(s) D(s)^{-1/2}$ where $D(s)$ is a diagonal matrix whose diagonals are node degrees, or random walk normalized Laplacian $L_{\text{rw}}(s) = I - D(s)^{-1} A(s)$. The objective (3) is understood as the the ordinary HIPPO approximation objective augmented with a regularization component that encourages the smoothness of memory compression with respect to adjacent nodes. The imposition of smoothness constraints commonly emerges as a beneficial relational inductive bias in the context of graph learning [1]. By leveraging the data from adjacent nodes, one can potentially achieve a more effective denoising effect during the process of node memory compression.

Remark 1 (A simultaneous compression perspective). *Alternatively, we may regard the objective (3) as comprising two tasks that simultaneously do the feature compression and the graph compression,*

²Technically, we require Z and X to reside within some appropriately defined Hilbert space. A comprehensive treatment will be provided in appendix C.

with the later task expressed through the Laplacian quadratic form. Specifically, as $\alpha \rightarrow \infty$ and pick $L = L_{\text{sym}}$ as the symmetric Laplacian. The solution of (3) is then given by a piecewise-constant vector that encodes the degree profile over connected components of the underlying graph. We provide a comprehensive discussion on compression semantics reflected through difference choice of Laplacians in appendix B.1.

To specify a suitable approximation subspace for memories Z , we adopt the approach of HiPPO that uses some N -dimensional subspace of polynomials which we denote as \mathcal{P}_N . Now we define a *graph memory projection operator* GPROJ_t that maps the temporal graph up until time t to a collection of N_V polynomials with each one lies in \mathcal{P}_N , i.e.,

$$\text{GPROJ}_t(G, X) = \arg \min_{Z: z_v \in \mathcal{P}_N \ \forall v \in V} \mathcal{L}_t(Z; G, X, \mu). \quad (4)$$

We further define a *coefficient operator* COEF_t that maps each polynomial in the collection in (4) to the coefficients of the basis of orthogonal polynomials defined with respect to μ_t , the following definition formalizes our extension of HiPPO to continuous-time temporal graphs which we term GHIPPO:

Definition 1 (GHIPPO). *Given a continuous-time temporal graph (G, X) , a time-varying measure family μ_t , an N -dimensional subspace of polynomials \mathcal{P}_N , the GHIPPO operator at time t is the composition of GPROJ_t and COEF_t that maps the temporal graph and node features to a collection of projection coefficients $U(t) \in \mathbb{R}^{N_V \times N}$, or $\text{GHIPPO}(G, X) = \text{COEF}_t(\text{GPROJ}_t(G, X))$.*

The most favorable property of the HiPPO framework on independent inputs is that the outputs of HiPPO operators are characterized via a concise ordinary differential equation (ODE) that takes the form of a linear time-invariant state-space model (LTI-SSM). The following theorem states that most of the desirable properties of HiPPO is retained by GHIPPO except for the LTI property:

Theorem 1. *Let G evolve according to (2). Taking μ_t to be the scaled Legendre measure (LegS) with $\mu_t = \frac{1}{t} \mathbb{I}_{[0, t]}$ where $\mathbb{I}_{[0, t]}$ stands for the indicator function of the interval $[0, t]$, the evolution of the outputs of GHIPPO operator is characterized by M ODEs according to mutation times as follows:*

$$\frac{dU(t)}{dt} = U(t)A^\top + (I + \alpha L(t))^{-1}X(t)B^\top, \quad 1 \leq m \leq M, t \in [t_{m-1}, t_m) \quad (5)$$

where $A \in \mathbb{R}^{N \times N}$ and $B \in \mathbb{R}^{N \times 1}$ takes the same form as in the HiPPO formulation [11]:

$$A_{nk} = - \begin{cases} \sqrt{(2n+1)(2k+1)} & \text{if } n > k, \\ n+1 & \text{if } n = k, \\ 0 & \text{if } n < k, \end{cases} \quad \text{and} \quad B_n = \sqrt{2n+1}, 1 \leq n \leq N. \quad (6)$$

According to theorem 1, the solution (5) is LTI over each interval $[t_m, t_{m+1})$ during which the graph structure remains fixed. This property further extends to a piecewise LTI perspective over the interval $[0, T]$. Moreover, we may view the solution (5) as a two-stage procedure that could be intuitively described as *diffuse-then-update*. Specifically, this procedure entails a sequential execution, wherein an initial diffusion operation is applied to the features of the input nodes, succeeded by an update to the memory of these nodes.

3.2 Unobserved graph mutations and mixed discretization

Theorem 1 establishes an analogue of HiPPO theory on temporal graphs. It is straightforward to verify that most of the subsequent refinements of HiPPO applies to GHIPPO as well. Among which we will utilize the popular technique of *diagonal state spaces* [15, 12] that simply sets A as a diagonal matrix with negative diagonal elements.³ To apply the GHIPPO framework to discrete-time temporal graphs, a critical step is to develop a discretized version of (5). However, unlike ordinary HiPPO where we can use standard discretization techniques of ODEs to discretize LTI equations, the GHIPPO ODE contains discontinuities that corresponds to mutation times of the underlying temporal graph, which are often not observed given only access to a list of snapshots. This issue of

³More concretely, diagonal SSMs are defined by diagonal A matrices whose diagonal elements are lying on the complex plane with negative real parts. [12], yet recent developments have found that complex state matrices are often not necessary [10]. For ease of representation, we only explore real state matrices in this paper.

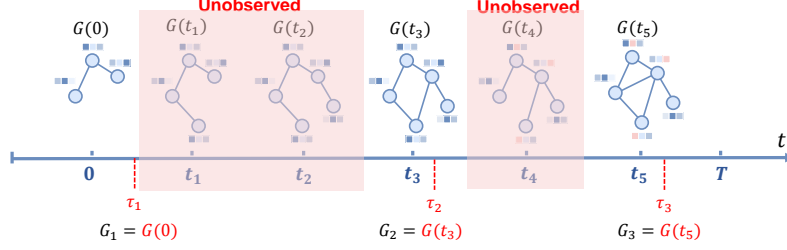


Figure 2: Illustrative example of the *unobserved graph mutation* issue. In this example, the underlying graph is observed at time points τ_1, τ_2, τ_3 with two unobserved mutations between $[\tau_1, \tau_2)$ and one between $[\tau_2, \tau_3)$. These unobserved mutations result in temporal dynamics that are inconsistent across the observed intervals, thereby complicating direct applications of ODE discretization methods such as the Euler method or zero-order hold (ZOH) method.

unobserved dynamics complicates the development of a viable discretization scheme for GHIPPO, as is pictorially illustrated in figure 2. To devise a solution to this challenge, we start by analyzing a hypothetical *oracle scenario* in which all mutations are observable.

An oracle discretization We consider a time range $[\tau_{l-1}, \tau_l)$ between the $l-1$ th and the l th snapshot, and assume there are altogether M_l mutation events $\{\mathcal{E}_{l,i}\}_{1 \leq i \leq M_l}$ happened during this period. Let $G_{l,0} = G_{l-1}$ be the graph snapshot at τ_{l-1} , the following process describes the structural evolution inside the interval $[\tau_{l-1}, \tau_l)$:

$$G_{l-1} = G_{l,0} \xrightarrow{\mathcal{E}_{l,1}} G_{l,1} \xrightarrow{\mathcal{E}_{l,2}} G_{l,2} \longrightarrow \cdots \longrightarrow G_{l,M_l-1} \xrightarrow{\mathcal{E}_{l,M_l}} G_{l,M_l} = G_l \quad (7)$$

Next we derive a discretization formula under the strategy of zeroth-order-hold (ZOH). We assume that all the intermediate mutations are observed, with the node features stay fixed between mutations, i.e., $X(t) \equiv X_{l,i}, t \in [t_{l,i-1}, t_{l,i})$. The following theorem characterizes the resulting state evolution:

Theorem 2 (Oracle discretization of (9)). *Assume A is a diagonal matrix with negative diagonals, for any $1 \leq l \leq L$. Let $L_{l,i}$ be some Laplacian of $G_{l,i}$, we have the following oracle update rule:*

$$U_l = U_{l-1} e^{\Delta_l A} + \tilde{X}_l (e^{\Delta_l A} - I) A^{-1}, \quad \tilde{X}_l = \sum_{i=0}^{M_l} (I + \alpha L_{l,i})^{-1} X_{l,i} \Lambda_i B^\top, \quad (8)$$

where $U_l \in \mathbb{R}^{N_v \times N}$ denotes the discretized state at step l with $U_0 = 0$. For each $1 \leq l \leq L, 0 \leq i \leq M_l$, $\Lambda_i \in \mathbb{R}^{N \times N}$ are non-negative diagonal matrices with values depending only on the mutation times, which satisfy $\sum_{i=0}^{M_l} \Lambda_i = I$.

Mixed discretization According to (8), given all the (unobserved) mutation information, the state update rule is equivalent to applying ZOH to \tilde{X}_l which is an *element-wise convex combination* of all the diffused node features. In practice, among all the components of \tilde{X} , we only have access to $X_{l-1}, X_l, G_{l-1}, G_l$ with the rest left unobserved. Therefore, we propose *mixed discretization* as an approach to approximate \tilde{X}_l . Specifically, we introduce the following mechanisms:

$$\hat{X}_l^{(O)} = \text{GNN}_\theta(X_l, G_l), \quad (\text{ordinary ZOH})$$

$$\hat{X}_l^{(F)} = \text{GNN}_\theta(\text{MIX}_\phi(X_{l-1}, X_l), G_l), \quad (\text{feature mixing})$$

$$\hat{X}_l^{(R)} = \text{MIX}_\phi(\text{GNN}_\theta(X_{l-1}, G_{l-1}), \text{GNN}_\theta(X_l, G_l)), \quad (\text{representation mixing})$$

which are compositions of inter-node mixing (a consequence of diffusion) and intra-node mixing (mixing node features of consecutive snapshots). For the process of inter-node mixing, we opt to approximate the diffusion operation with a learnable shallow graph neural network (typically a 1-layer GNN) parameterized by θ to alleviate the computation burden and improve flexibility.⁴ A detailed discussion considering the relation between certain GNN formulation and the choice of Laplacian is presented in appendix B.1. In the context of intra-node mixing, we introduce a MIX module parameterized by ϕ to merge either consecutive node features (as illustrated in (feature mixing)) or consecutive

⁴We let the balancing constant α be absorbed into the learnable parameters. Indeed, for GNNs that employ asymmetric aggregation [16], it is plausible to conceptualize the GNN as engaging a form of auto-balancing.

node representations produced by the GNN model (as illustrated in (representation mixing)). In this paper we assess two simple MIX instantiations: Convolution with a kernel size of 2 (CONV1D) and a gating mechanism that interpolates between the two inputs (INTERP). We postpone a comprehensive description of the mixing methods to appendix D.1. The resulting discretized system is presented as the following matrix-valued state space model:

$$\begin{aligned} U_l &= U_{l-1}e^{\Delta_l A} + \Delta_l \hat{X}_l^{(\cdot)} B^\top \quad \text{with} \quad \hat{X}_l^{(\cdot)} \in \left\{ \hat{X}_l^{(O)}, \hat{X}_l^{(F)}, \hat{X}_l^{(R)} \right\}, 1 \leq l \leq L. \\ Y_l &= U_l C^\top. \end{aligned} \quad (9)$$

When exact timestamps for snapshots are unavailable, we use the adaptive time step strategy as in [11, 10] that models Δ a 1-dimensional affine projection of the inputs followed by a non-negative activation like softplus. Finally, we utilize the approximation $A^{-1}(e^{\Delta A} - I) \approx \Delta I$ for diagonal A s, and equip the system with an output Y with a state projection matrix $C \in \mathbb{R}^{N \times 1}$.

3.3 The GRAPHSSM framework

Having established the SSM equation (9), we are ready to introduce our main framework GRAPHSSM. In alignment with conventional design paradigms in the SSM literature, we define a depth- K GRAPHSSM model through the sequential composition of K GRAPHSSM blocks, with each block characterized as follows:

$$H_{1:L}^{(k)} = \sigma \left(\text{SSMLAYER} \left(H_{1:L}^{(k-1)}, G_{1:L} \right) \right) + \text{lin} \left(H_{1:L}^{(k-1)} \right), 1 \leq k \leq K, \quad (10)$$

where we use $H_{1:L}^{(k)}$ to denote the concatenation of the hidden representation at depth k of all the snapshots along the sequence dimension and $H_{1:L}^{(0)}$ are the node features $X_{1:L}$. The GRAPHSSM blocks, as outlined in (10), incorporate an SSM layer that operates on graph snapshot inputs. This is followed by the application of a nonlinear activation σ and the integration of a residual connection which we denote has the addition of a linear projection of inputs with lin denotes a linear projection layer that ensures dimension compatibility.

GRAPHSSM-S4 The architectural formulation of the SSM layer essentially involves the expansion of the one-dimensional recurrence, as specified in (9), to accommodate general dimensions, i.e., $d > 1$. This expansion is achieved in a straightforward manner by utilizing an individual SSM for each dimension. Consequently, the emergent SSM layer adopts a Single-Input, Single-Output (SISO) configuration. Such a design is intuitively understood as the graph learning analogue of S4 [13] which we term GRAPHSSM-S4.

GRAPHSSM-S5 and GRAPHSSM-S6 In addition to the SISO implementation, we further introduce two variants within the GRAPHSSM framework. The first alternative represents a Multiple-Input, Multiple-Output (MIMO) extension of (9), wherein a single SSM system is applied across all dimensions. This variant serves as a graph-informed analogue to the S5 model [39]. The second variant extends the S4 model by facilitating input-controlled time intervals and state matrices (Δ , B , and C). This innovation yields a selective state space model, drawing parallels to latest SSM architectures such as S6 [10].

A detailed exposition of the GRAPHSSM-S4 (resp. GRAPHSSM-S5, GRAPHSSM-S6) layer is provided in algorithm 1 (resp. algorithm 2, algorithm 3) in appendix D.2. The overall end-to-end architecture is succinctly illustrated in figure 1, where we use feature mixing as the mixing mechanism for illustration.

Remark 2 (Choice of mixing mechanisms). *In the GRAPHSSM architecture, each SSM layer incorporates a mixing mechanism. Based on our empirical investigations, we have observed that employing more sophisticated mixing strategies such as (feature mixing) and (representation mixing), yields benefits predominantly when these are applied exclusively to the lowermost layer. Specifically, this entails utilizing either $\hat{X}_l^{(F)}$ or $\hat{X}_l^{(R)}$ configurations in the initial layer, while defaulting to $\hat{X}_l^{(O)}$ for the layers that follow. An intuitive rationale behind this strategic layer-specific choice will be elucidated in appendix B.3.*

4 Experiments

This section presents our key experimental findings on the temporal node classification task. Also, ablation studies of the key design choices are presented. Due to space limitation, the detailed experi-

mental settings are deferred in appendix F. The source code of GRAPHSSM, including datasets and all the code for reproducing the results is made available in the supplementary material accompanying the submission.

Table 2: Node classification performance (%) on four small scale temporal graphs. The best and the second best results are highlighted as **red** and **blue**, respectively.

	DBLP-3		Brain		Reddit		DBLP-10	
	Micro-F1	Macro-F1	Micro-F1	Macro-F1	Micro-F1	Macro-F1	Micro-F1	Macro-F1
DeepWalk [35]	47.53 \pm 0.4	47.21 \pm 0.2	51.45 \pm 0.6	51.03 \pm 0.8	26.82 \pm 0.6	26.75 \pm 0.4	66.38	67.12
Node2Vec [9]	48.79 \pm 0.3	48.42 \pm 0.4	53.51 \pm 0.5	52.95 \pm 0.6	25.47 \pm 0.6	25.44 \pm 0.5	67.31	66.93
HTNE [52]	48.98 \pm 0.2	48.74 \pm 0.3	22.31 \pm 0.8	22.12 \pm 0.5	26.96 \pm 0.5	26.80 \pm 0.7	68.79	68.36
M ² DNE [27]	49.12 \pm 0.5	48.87 \pm 0.4	23.79 \pm 0.5	23.54 \pm 0.6	25.79 \pm 0.6	25.61 \pm 0.4	69.71	69.75
DynamicTriad [48]	48.78 \pm 0.5	48.63 \pm 0.6	21.71 \pm 0.7	21.94 \pm 0.7	28.76 \pm 0.5	28.51 \pm 0.5	66.95	66.42
MPNN [31]	81.78 \pm 0.6	81.46 \pm 1.2	90.97 \pm 1.4	91.01 \pm 1.5	40.85 \pm 1.3	40.64 \pm 1.2	67.74 \pm 0.3	65.05 \pm 0.5
STAR [45]	84.74 \pm 1.0	84.20 \pm 1.2	92.08 \pm 1.3	92.23 \pm 1.3	43.42 \pm 2.3	43.43 \pm 2.4	72.98 \pm 1.5	72.03 \pm 1.2
tNodeEmbed [38]	84.51 \pm 1.2	83.57 \pm 1.1	92.35 \pm 0.8	92.30 \pm 1.0	42.11 \pm 1.8	42.06 \pm 1.3	74.19 \pm 1.8	74.23 \pm 2.2
EvolveGCN [33]	84.01 \pm 1.5	83.12 \pm 1.5	92.20 \pm 1.3	92.00 \pm 1.0	41.24 \pm 1.3	41.11 \pm 1.5	71.32 \pm 0.5	71.20 \pm 0.7
SpikeNet [24]	83.92 \pm 1.5	83.04 \pm 1.1	92.00 \pm 1.2	91.97 \pm 1.2	40.42 \pm 2.0	40.20 \pm 2.1	74.86 \pm 0.5	74.65 \pm 0.5
ROLAND [46]	84.21 \pm 1.4	84.06 \pm 1.5	92.14 \pm 1.2	91.85 \pm 1.14	44.22 \pm 2.2	44.25 \pm 1.9	75.01 \pm 1.1	74.98 \pm 1.0
GRAPHSSM	85.26 \pm 0.9	85.00 \pm 1.3	93.52 \pm 1.0	93.54 \pm 0.9	49.21 \pm 0.5	49.05 \pm 0.7	76.80 \pm 0.3	76.00 \pm 0.4

4.1 Experimental results

Node classification performance. The node classification performance of all methods are presented in Table 2. It has been observed that graph embedding methods, especially static ones, tend to underperform in most cases. This is expected since these methods are typically trained in an unsupervised manner, solely focusing on exploiting the graph structure. We note that continuous-time methods HTNE and M² exhibit poor performance in DBLP-3, Brain and Reddit even when compared to static methods. This indicates that continuous-time methods are not well-suited for handling discrete-time graphs, particularly in the absence of temporal continuity. As can be also observed from Table 2, most temporal graph neural networks demonstrate good performance on DBLP-3 and Brain datasets, where the node labels are largely dominated by node attribute information [45]. However, for datasets like Reddit and DBLP-10, where graph topology information plays a more significant role in classification, the performance has notably degraded. This indicates that the baseline methods struggle to effectively capture the underlying evolving graph structure and exploit it for accurate classification. In contrast, our most performant architecture, GRAPHSSM-S4, exhibits an average improvement of 14% and 2% in Micro-F1 and Macro-F1 scores, respectively, compared to state-of-the-art baselines on the Reddit and DBLP-10 datasets. In addition, GRAPHSSM-S4 is a more preferable choice for long graph sequences, achieving new state-of-the-art performance on the DBLP-10 dataset.

Scalability to large temporal graphs. To explore the effectiveness of GRAPHSSM on large scale and long-range temporal graphs, we conduct comparison experiments on arXiv and Tmall and present the result in Table 3. Since both datasets exhibit a relatively high level of temporal continuity in the observed graph sequence, several advanced baselines have achieved good performance. However, the graph scale and long sequence still pose significant challenges for learning over both datasets, where most methods are insufficient to effectively and efficiently capture the long-range graph dynamics. In contrast, by leveraging the linear efficiency and long-range modeling capability of SSMs, GRAPHSSM outperforms strong baselines on both datasets.

Table 3: Node classification performance (%) on large scale temporal graphs. OOM: out-of-memory.

	arXiv		Tmall	
	Micro-F1	Macro-F1	Micro-F1	Macro-F1
DeepWalk [35]	66.54 \pm 0.3	43.01 \pm 0.3	57.88	49.53
Node2Vec [9]	67.71 \pm 0.5	43.69 \pm 0.4	60.66	54.58
HTNE [52]	65.48 \pm 0.3	42.25 \pm 0.3	62.64	54.93
M ² DNE [27]	66.91 \pm 0.5	43.52 \pm 0.6	64.65	58.47
DynamicTriad [48]	61.10 \pm 0.2	38.25 \pm 0.3	60.72	51.16
MPNN [31]	64.68 \pm 1.7	41.22 \pm 1.5	58.07 \pm 0.6	50.27 \pm 0.5
STAR [45]	OOM	OOM	OOM	OOM
tNodeEmbed [38]	OOM	OOM	OOM	OOM
EvolveGCN [33]	65.17 \pm 1.4	43.01 \pm 1.3	61.77 \pm 0.6	55.78 \pm 0.6
SpikeNet [24]	66.69 \pm 0.9	43.96 \pm 1.0	66.10 \pm 0.3	62.40 \pm 0.6
ROLAND [46]	68.27 \pm 1.2	48.01 \pm 1.3	OOM	OOM
GRAPHSSM	70.67 \pm 0.7	49.97 \pm 0.5	66.29 \pm 0.1	62.57 \pm 0.1

Table 4: Node classification performance (%) with different SSM architectures.

	DBLP-3		Brain		Reddit		DBLP-10	
	Micro-F1	Macro-F1	Micro-F1	Macro-F1	Micro-F1	Macro-F1	Micro-F1	Macro-F1
GRAPHSSM-S4	85.26 \pm 0.9	85.00 \pm 1.3	93.52 \pm 1.0	93.54 \pm 0.9	49.21 \pm 0.5	49.05 \pm 0.7	76.80 \pm 0.3	76.00 \pm 0.4
GRAPHSSM-S5	86.29 \pm 1.0	85.78 \pm 0.9	93.00 \pm 0.4	93.01 \pm 0.4	44.75 \pm 0.4	44.79 \pm 0.4	75.19 \pm 0.6	73.95 \pm 0.4
GRAPHSSM-S6	86.10 \pm 0.5	85.70 \pm 0.6	93.80 \pm 0.3	94.47 \pm 0.6	43.11 \pm 0.9	42.85 \pm 1.1	74.09 \pm 0.3	73.16 \pm 0.2

SSM architectures. As GRAPHSSM is a general framework that generalize SSMs to temporal graphs, we conduct experiments on extending GRAPHSSM with different ad-hoc SSMs, including S5 [39] and S6 [10]. The node classification results on four datasets are shown in Table 4. By comparing different variants of GRAPHSSM, we can find that S4 is the best architecture to learning over temporal graph sequences. S5, being a simplified version of S4 with fewer parameters, achieves poor performance on all datasets. Notably, while S6 are shown impressive performance in other modalities such as language or images [10, 49], it is observed that they underperform when applied to graph sequences. This indicates that the selective mechanism may not be a good fit for graph data.

Table 5: Ablation results (%) of GRAPHSSM-S4 with different mixing configurations.

	DBLP-3		Brain		Reddit		DBLP-10	
	Micro-F1	Macro-F1	Micro-F1	Macro-F1	Micro-F1	Macro-F1	Micro-F1	Macro-F1
$\hat{X}_1^{(O)} + \hat{X}_2^{(O)}$	84.51 \pm 0.9	84.28 \pm 0.9	91.56 \pm 1.1	91.99 \pm 0.7	48.05 \pm 2.8	47.99 \pm 3.0	75.62 \pm 0.5	74.65 \pm 0.6
$\hat{X}_1^{(F)} + \hat{X}_2^{(O)}$	85.12 \pm 0.5	84.82 \pm 0.3	92.36 \pm 0.8	92.54 \pm 0.9	49.06 \pm 1.9	49.06 \pm 1.8	76.67 \pm 0.6	75.95 \pm 0.7
$\hat{X}_1^{(R)} + \hat{X}_2^{(O)}$	84.98 \pm 1.1	84.79 \pm 1.0	93.52 \pm 1.0	93.54 \pm 0.9	49.21 \pm 0.5	49.05 \pm 0.7	77.76 \pm 0.5	77.54 \pm 0.6
$\hat{X}_1^{(O)} + \hat{X}_2^{(R)}$	85.26 \pm 0.9	85.00 \pm 1.3	91.84 \pm 1.9	91.88 \pm 1.7	47.88 \pm 1.8	47.94 \pm 1.8	75.41 \pm 0.7	74.89 \pm 1.0

Mixing mechanism. We assess the effectiveness of various mixing mechanisms introduced in section 3.2 through a series of experiments conducted using the S4 variant of GRAPHSSM. The analysis spans four distinct configurations: no intra-node mixing ($\hat{X}_1^{(O)} + \hat{X}_2^{(O)}$), **feature mixing** at the first layer ($\hat{X}_1^{(F)} + \hat{X}_2^{(O)}$), and **representation mixing** at either the first ($\hat{X}_1^{(R)} + \hat{X}_2^{(O)}$) or second ($\hat{X}_1^{(O)} + \hat{X}_2^{(R)}$) layers. The findings, presented in Table 5, indicate that the integration of the MIX module at the first layer generally leads to enhanced model performance. An intuitive explanation for this observed phenomenon is elaborated in appendix B.3.

Initialization strategy. Recent advancements have highlighted the crucial role of initialization in SSMs [12], prompting our investigation into the effects of various initialization strategies for the A matrix. Specifically, we explore "hippo", "constant", and "random" initializations, with their comprehensive definitions provided in appendix D.2. The result, as shown in Figure 3 exhibits distinct performance variations across different initialization strategies, with HIPPO being typically the dominant one which corroborates our theoretical motivations.

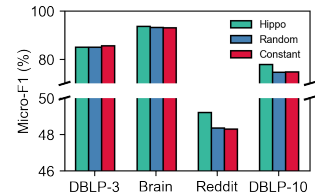


Figure 3: Comparison of GRAPHSSM with different initialization strategies.

5 Conclusion

In this work, we introduce a conceptualized GHIPPO abstraction on temporal graphs. Building upon GHIPPO, we propose GRAPHSSM, a theoretically motivated state space framework for modeling temporal graphs derived from a novel memory compression scheme. The proposed framework is and computationally efficient and versatile in its design, which is further corroborated by strong empirical performance across various benchmark datasets. We also point out the unobserved graph mutation issue in temporal graphs and propose different mixing mechanisms to ensure temporal continuity. Despite the promising results, the applicability of GRAPHSSM is presently confined to discrete-time temporal graphs. A discussion of our framework's current limitations and the scope for future extensions is presented in appendix E.

References

- [1] P. W. Battaglia, J. B. Hamrick, V. Bapst, A. Sanchez-Gonzalez, V. Zambaldi, M. Malinowski, A. Tacchetti, D. Raposo, A. Santoro, R. Faulkner, et al. Relational inductive biases, deep learning, and graph networks. *arXiv preprint arXiv:1806.01261*, 2018.
- [2] A. Behrouz and F. Hashemi. Graph mamba: Towards learning on graphs with state space models. *CoRR*, abs/2402.08678, 2024.
- [3] P. J. Brockwell and R. A. Davis. *Time series: theory and methods*. Springer science & business media, 1991.
- [4] K. Cho, B. van Merriënboer, Ç. Gülçehre, D. Bahdanau, F. Bougares, H. Schwenk, and Y. Bengio. Learning phrase representations using RNN encoder-decoder for statistical machine translation. In *EMNLP*, pages 1724–1734. ACL, 2014.
- [5] M. Fey and J. E. Lenssen. Fast graph representation learning with PyTorch Geometric. In *ICLR Workshop on Representation Learning on Graphs and Manifolds*, 2019.
- [6] D. Y. Fu, T. Dao, K. K. Saab, A. W. Thomas, A. Rudra, and C. Ré. Hungry hungry hippos: Towards language modeling with state space models. In *ICLR*. OpenReview.net, 2023.
- [7] D. Y. Fu, H. Kumbong, E. Nguyen, and C. Ré. Flashfftconv: Efficient convolutions for long sequences with tensor cores. *arXiv preprint arXiv:2311.05908*, 2023.
- [8] W. Gerstner, W. M. Kistler, R. Naud, and L. Paninski. *Neuronal dynamics: From single neurons to networks and models of cognition*. Cambridge University Press, 2014.
- [9] A. Grover and J. Leskovec. node2vec: Scalable feature learning for networks. In *KDD*, pages 855–864. ACM, 2016.
- [10] A. Gu and T. Dao. Mamba: Linear-time sequence modeling with selective state spaces. *CoRR*, abs/2312.00752, 2023.
- [11] A. Gu, T. Dao, S. Ermon, A. Rudra, and C. Ré. Hippo: Recurrent memory with optimal polynomial projections. In *NeurIPS*, 2020.
- [12] A. Gu, K. Goel, A. Gupta, and C. Ré. On the parameterization and initialization of diagonal state space models. *Advances in Neural Information Processing Systems*, 35:35971–35983, 2022.
- [13] A. Gu, K. Goel, and C. Ré. Efficiently modeling long sequences with structured state spaces. In *ICLR*. OpenReview.net, 2022.
- [14] A. Gu, I. Johnson, K. Goel, K. Saab, T. Dao, A. Rudra, and C. Ré. Combining recurrent, convolutional, and continuous-time models with linear state space layers. In *NeurIPS*, pages 572–585, 2021.
- [15] A. Gupta, A. Gu, and J. Berant. Diagonal state spaces are as effective as structured state spaces. *Advances in Neural Information Processing Systems*, 35:22982–22994, 2022.
- [16] W. Hamilton, Z. Ying, and J. Leskovec. Inductive representation learning on large graphs. *Advances in neural information processing systems*, 30, 2017.
- [17] F. Hashemi, A. Behrouz, and M. R. Hajidehi. CS-TGN: community search via temporal graph neural networks. In *WWW (Companion Volume)*, pages 1196–1203. ACM, 2023.
- [18] S. Hochreiter and J. Schmidhuber. Long short-term memory. *Neural Comput.*, 9(8):1735–1780, 1997.
- [19] W. Hu, M. Fey, M. Zitnik, Y. Dong, H. Ren, B. Liu, M. Catasta, and J. Leskovec. Open graph benchmark: Datasets for machine learning on graphs. In *NeurIPS*, 2020.
- [20] S. M. Kazemi, R. Goel, K. Jain, I. Kobyzev, A. Sethi, P. Forsyth, and P. Poupart. Representation learning for dynamic graphs: A survey. *J. Mach. Learn. Res.*, 21(1), jan 2020.
- [21] S. M. Kazemi, R. Goel, K. Jain, I. Kobyzev, A. Sethi, P. Forsyth, and P. Poupart. Representation learning for dynamic graphs: A survey. *J. Mach. Learn. Res.*, 21:70:1–70:73, 2020.
- [22] T. N. Kipf and M. Welling. Semi-supervised classification with graph convolutional networks. In *ICLR (Poster)*. OpenReview.net, 2017.
- [23] S. Kumar, X. Zhang, and J. Leskovec. Predicting dynamic embedding trajectory in temporal interaction networks. In *KDD*, pages 1269–1278. ACM, 2019.

- [24] J. Li, Z. Yu, Z. Zhu, L. Chen, Q. Yu, Z. Zheng, S. Tian, R. Wu, and C. Meng. Scaling up dynamic graph representation learning via spiking neural networks. In *AAAI*, pages 8588–8596. AAAI Press, 2023.
- [25] J. Li, H. Zhang, R. Wu, Z. Zhu, B. Wang, C. Meng, Z. Zheng, and L. Chen. A graph is worth 1-bit spikes: When graph contrastive learning meets spiking neural networks. In *ICLR*, 2024.
- [26] A. Longa, V. Lachi, G. Santin, M. Bianchini, B. Lepri, P. Liò, F. Scarselli, and A. Passerini. Graph neural networks for temporal graphs: State of the art, open challenges, and opportunities. *CoRR*, abs/2302.01018, 2023.
- [27] Y. Lu, X. Wang, C. Shi, P. S. Yu, and Y. Ye. Temporal network embedding with micro- and macro-dynamics. In *CIKM*, pages 469–478. ACM, 2019.
- [28] E. Nguyen, K. Goel, A. Gu, G. W. Downs, P. Shah, T. Dao, S. Baccus, and C. Ré. S4ND: modeling images and videos as multidimensional signals with state spaces. In *NeurIPS*, 2022.
- [29] A. V. Oppenheim, J. Buck, M. Daniel, A. S. Willsky, S. H. Nawab, and A. Singer. *Signals & systems*. Pearson Education, 1997.
- [30] A. Orvieto, S. L. Smith, A. Gu, A. Fernando, C. Gulcehre, R. Pascanu, and S. De. Resurrecting recurrent neural networks for long sequences. In *International Conference on Machine Learning*, pages 26670–26698. PMLR, 2023.
- [31] G. Panagopoulos, G. Nikolentzos, and M. Vazirgiannis. Transfer graph neural networks for pandemic forecasting. In *AAAI*, pages 4838–4845. AAAI Press, 2021.
- [32] J. Pang and G. Cheung. Graph laplacian regularization for image denoising: Analysis in the continuous domain. *IEEE Transactions on Image Processing*, 26(4):1770–1785, 2017.
- [33] A. Pareja, G. Domeniconi, J. Chen, T. Ma, T. Suzumura, H. Kanezashi, T. Kaler, T. B. Schardl, and C. E. Leiserson. Evolvegc: Evolving graph convolutional networks for dynamic graphs. In *AAAI*, pages 5363–5370. AAAI Press, 2020.
- [34] A. Paszke, S. Gross, F. Massa, A. Lerer, J. Bradbury, G. Chanan, T. Killeen, Z. Lin, N. Gimelshein, L. Antiga, A. Desmaison, A. Köpf, E. Z. Yang, Z. DeVito, M. Raison, A. Tejani, S. Chilamkurthy, B. Steiner, L. Fang, J. Bai, and S. Chintala. Pytorch: An imperative style, high-performance deep learning library. In *NeurIPS*, pages 8024–8035, 2019.
- [35] B. Perozzi, R. Al-Rfou, and S. Skiena. Deepwalk: online learning of social representations. In *KDD*, pages 701–710. ACM, 2014.
- [36] A. Rogozhnikov. Einops: Clear and reliable tensor manipulations with einstein-like notation. In *International Conference on Learning Representations*, 2022.
- [37] E. Salinas and T. J. Sejnowski. Integrate-and-fire neurons driven by correlated stochastic input. *Neural computation*, 14(9):2111–2155, 2002.
- [38] U. Singer, I. Guy, and K. Radinsky. Node embedding over temporal graphs. In *IJCAI*, pages 4605–4612. ijcai.org, 2019.
- [39] J. T. H. Smith, A. Warrington, and S. W. Linderman. Simplified state space layers for sequence modeling. In *ICLR*. OpenReview.net, 2023.
- [40] A. Vaswani, N. Shazeer, N. Parmar, J. Uszkoreit, L. Jones, A. N. Gomez, L. Kaiser, and I. Polosukhin. Attention is all you need. In *NIPS*, pages 5998–6008, 2017.
- [41] P. Velickovic, G. Cucurull, A. Casanova, A. Romero, P. Liò, and Y. Bengio. Graph attention networks. In *ICLR (Poster)*. OpenReview.net, 2018.
- [42] Y. Wang, Y. Chang, Y. Liu, J. Leskovec, and P. Li. Inductive representation learning in temporal networks via causal anonymous walks. In *ICLR*. OpenReview.net, 2021.
- [43] C. Wei, K. Shen, Y. Chen, and T. Ma. Theoretical analysis of self-training with deep networks on unlabeled data. *arXiv preprint arXiv:2010.03622*, 2020.
- [44] R. J. Williams and D. Zipser. A learning algorithm for continually running fully recurrent neural networks. *Neural Comput.*, 1(2):270–280, 1989.
- [45] D. Xu, W. Cheng, D. Luo, X. Liu, and X. Zhang. Spatio-temporal attentive RNN for node classification in temporal attributed graphs. In *IJCAI*, pages 3947–3953. ijcai.org, 2019.
- [46] J. You, T. Du, and J. Leskovec. ROLAND: graph learning framework for dynamic graphs. In *KDD*, pages 2358–2366. ACM, 2022.

- [47] M. Zhang, K. K. Saab, M. Poli, T. Dao, K. Goel, and C. Ré. Effectively modeling time series with simple discrete state spaces. *arXiv preprint arXiv:2303.09489*, 2023.
- [48] L. Zhou, Y. Yang, X. Ren, F. Wu, and Y. Zhuang. Dynamic network embedding by modeling triadic closure process. In *AAAI*, pages 571–578. AAAI Press, 2018.
- [49] L. Zhu, B. Liao, Q. Zhang, X. Wang, W. Liu, and X. Wang. Vision mamba: Efficient visual representation learning with bidirectional state space model. *CoRR*, abs/2401.09417, 2024.
- [50] X. Zhu, Z. Ghahramani, and J. D. Lafferty. Semi-supervised learning using gaussian fields and harmonic functions. In *Proceedings of the 20th International conference on Machine learning (ICML-03)*, pages 912–919, 2003.
- [51] Y. Zhu, F. Cong, D. Zhang, W. Gong, Q. Lin, W. Feng, Y. Dong, and J. Tang. Wingnn: Dynamic graph neural networks with random gradient aggregation window. In *KDD*, pages 3650–3662. ACM, 2023.
- [52] Y. Zuo, G. Liu, H. Lin, J. Guo, X. Hu, and J. Wu. Embedding temporal network via neighborhood formation. In *KDD*, pages 2857–2866. ACM, 2018.

Appendix

Table of Contents

A Broader impact	13
B Notes	13
B.1 Laplacian regularization, diffusion and GNN approximation	13
B.2 An extension to varying node sets	14
B.3 Heuristic justifications for layer-specific choice of mixing mechanisms	15
C Proof of theorems	15
C.1 Proof of theorem 1	15
C.2 Proof of theorem 2	16
D Algorithm descriptions	17
D.1 The designs of mixing mechanism MIX	17
D.2 Details of GRAPHSSM	18
D.3 Complexity and implementations	19
E Discussions and limitations	20
E.1 Extension to continuous-time temporal graphs	20
E.2 Going beyond piecewise dynamics	20
F Experimental setup	21

A Broader impact

Our extension of state space models for temporal graph modeling may have broader impacts, particularly if applied to social, traffic, and financial networks which could affect individuals and society. While our work is fundamental and not tied to specific applications, the potential for misuse in surveillance, exacerbation of biases in algorithmic decision-making, or violation of privacy cannot be dismissed. For example, more accurate temporal graph models might inadvertently facilitate more intrusive tracking of individuals or groups, or could be employed in creating discriminatory financial models. It is the responsibility of those employing such technologies to consider these ethical implications and to implement measures such as algorithmic fairness checks, privacy-preserving methodologies, and security protocols that prevent exploitation of the technology. As with any powerful tool, the utmost caution should be exercised to avoid the irresponsible use of our advancements in modeling dynamic systems.

B Notes

B.1 Laplacian regularization, diffusion and GNN approximation

In this section, we discuss in detail the smoothness regularization of different types of Laplacians, and their approximations related to popular GNN architectures.

Inductive bias and compression capability of different Laplacians As mentioned in section 3.1, two typical (normalized) graph Laplacians are

$$L_{\text{sym}}(s) = I - D(s)^{-1/2} A(s) D(s)^{-1/2} \quad (11)$$

$$L_{\text{rw}}(s) = I - D(s)^{-1} A(s), \quad (12)$$

with corresponding penalties written as

$$\int_0^t Z(s)^\top L_{\text{sym}}(s) Z(s) d\mu_t(s) = \int_0^t \sum_{(u,v) \in E(s)} \left(\frac{z_u(s)}{\sqrt{d_u(s)}} - \frac{z_v(s)}{\sqrt{d_v(s)}} \right)^2 d\mu_t(s) \quad (13)$$

$$\int_0^t Z(s)^\top L_{\text{rw}}(s) Z(s) d\mu_t(s) = \int_0^t \sum_{(u,v) \in E(s)} \frac{1}{d_u} (z_u(s) - z_v(s))^2 d\mu_t(s). \quad (14)$$

The above display reveals the inductive bias of Laplacian regularizations as a promoting closeness in a weighted ℓ_2 metric regarding adjacent nodes' memory compressions, with distinct choices of Laplacians utilizing different weighting schemes. In particular, let $\alpha \rightarrow \infty$ in objective 3 then when the Laplacian is chosen as L_{sym} , the solution $Z^{\text{sym}}(s)$ must satisfy

$$\frac{z_v^{\text{sym}}(s)}{\sqrt{d_v(s)}} = \frac{z_u^{\text{sym}}(s)}{\sqrt{d_u(s)}}, \forall (u, v) \in E(s), 0 \leq s \leq t \quad (15)$$

It then follows that Z^{sym} compresses all the historical *degree profiles* over connected components of G . Analogously, when L_{rw} is chosen, it follows that the solution $Z^{\text{rw}}(s)$ must satisfy

$$z_v(s) = z_u(s), \forall (u, v) \in E(s), 0 \leq s \leq t \quad (16)$$

which compresses the composition of connected components of G .

Diffusion and GNN approximation We consider approximations of the following diffused node features with respect to some type of Laplacian:

$$H = \{h_v\}_{v \in V} := (I + \alpha L)^{-1} X B^\top = \left(I + \sum_{k=1}^{\infty} (-1)^k \alpha^k L^k \right) X B^\top \quad (17)$$

The right hand side of the preceding display is equivalent to performing infinite rounds of message passing. If we drop most of the higher-order terms, we arrive at models similar to graph neural networks. In particular, we keep only the first order terms, i.e., $k = 1$, then for the two Laplacians listed above, for each $v \in V$, we have the resulting approximations:

$$h_v^{\text{sym}} \approx (1 - \alpha) B x_v + \sum_{u \in N(v)} \frac{\alpha}{\sqrt{d_u d_v}} B f_u \quad (\text{GCN-Like})$$

$$h_v^{\text{rw}} \approx (1 - \alpha) B x_v + \sum_{u \in N(v)} \frac{\alpha}{d_u} B f_u. \quad (\text{SAGE(MEAN)-Like})$$

The above display exhibits a similar pattern to the design of graph neural networks with a aggregate-then-combine procedure, with the corresponding aggregation steps mirroring two typical GNN architectures GCN [22] and SAGE with mean pooling [16]. Furthermore, note that the effect of the balancing constant α would be absorbed into the learnable parameters of the GNN.

B.2 An extension to varying node sets

The methodology described in section 3.1 applies to temporal graphs with a *fixed* node set. To extend our approach to accommodate graphs featuring *varying* node sets, we initially focus on the continuous-time context, subsequently delving into discussions on discretization strategies. Suppose on the time interval $\mathcal{T} = [0, T]$, the node set evolves as depicted in the following sequence:

$$V(0) \longrightarrow V(t_1) \longrightarrow V(t_2) \longrightarrow \cdots \longrightarrow V(t_{R-1}) \longrightarrow V(t_R) = V(T). \quad (18)$$

That is, throughout the interval \mathcal{T} , the node set undergoes alterations on R distinct occasions, with associated changes occurring at times t_1, \dots, t_R , respectively. We denote these evolving node sets as V_0, \dots, V_R . To systematically analyze this temporal evolution, we partition the entire interval \mathcal{T} into $R + 1$ segments:

$$\mathcal{T}_r = [t_r, t_{r+1}), 0 \leq r \leq R \text{ with } t_0 = 0 \text{ and } t_{R+1} = T. \quad (19)$$

According to the formulations in section 3.1, on each \mathcal{T}_r , we have a well defined GHIPPO operator and the solutions are characterized by theorem 1. With an approximation order of N , we let the resulting projection coefficients be

$$U_r(t) \in \mathbb{R}^{|V_r| \times N}, 0 \leq r \leq R, t \in \mathcal{T}_r. \quad (20)$$

To address the issue of shape incoherence arising from variations in node sets, we employ a *memory alignment procedure*. This technique facilitates the mapping from $U_r(t_{r+1}-)$ to $U_{r+1}(t_{r+1})$, ensuring that the memory associated with each node is aligned according to the following scheme:

$$u_{v,r+1}(t_{r+1}) = \begin{cases} u_{v,r}(t_{r+1}-) & \text{if } v \in V_r \cap V_{r+1} \\ u_{\text{init}} & \text{if } v \in V_{r+1} \setminus V_r \end{cases}. \quad (21)$$

The memory alignment procedure (21) retains the continuity of states for nodes that persist over time. For nodes that emerge anew within the graph, it assigns a default initial state, which could either be an all-zero state or an estimation derived a priori from the states of neighboring nodes.

Discretizations Within the established context, Theorem 2 remains applicable on each segment \mathcal{T}_r . Consequently, our primary concern becomes the treatment of nodes that emerge between consecutive snapshots. Adhering to the ZOH discretization rule, newly emerged nodes lack historical states and therefore do not undergo the MIX strategy, and use their initial state during their first appearance in the recurrent update. This initial state can be set to zero or determined through aggregation from neighboring nodes.

B.3 Heuristic justifications for layer-specific choice of mixing mechanisms

The various mixing mechanisms introduced in this paper are designed to facilitate an estimation of a weighted average of unobserved graph representations that occur amidst successive observational time points. Starting with the output generated by the initial SSM block, these outputs inherently encapsulate the information pertaining to the current snapshot, as well as that of its antecedent. Thus, the incorporation of mixing mechanisms at a second-layer may inadvertently result in the assimilation of superfluous information, extending beyond the target scope of back-to-back snapshots. Therefore, confining the deployment of mixing solely to the first SSM layer ensures the strict conservation of temporal locality. We have empirically verified that such an approach yields enhanced performances.

C Proof of theorems

In this section we present the proof of theorem 1 and theorem 2. We first present some necessary technical preparations: For any $t \in [0, T]$, let μ_t be some finite measure and let \mathcal{H}_{μ_t} denote the Hilbert space induced by the inner product

$$\langle f, g \rangle_{\mu_t} := \int_0^t f(s)g(s)d\mu_t(s). \quad (22)$$

Let $\mathcal{P}_N(t)$ be the space of polynomials constructed via the restriction of each element in \mathcal{P}_N to $[0, t]$. We assume the measure family be chosen such that $\mathcal{P}_N(t) \subset \mathcal{H}_{\mu_t}, \forall t \in [0, T]$. For each $v \in V$, we assume that the restriction of x_v (viewing as a function on $[0, T]$) to $[0, t]$ is an element of \mathcal{H}_{μ_t} . Note that these assumptions are trivially satisfied for the scaled Legendre measure (LegS) $\mu_t = \frac{1}{t}\mathbb{I}_{[0,t]}$.

C.1 Proof of theorem 1

Proof of theorem 1. Hereafter we omit the dependence on μ_t and write the inner product simply as $\langle \cdot, \cdot \rangle$ without misunderstandings. Let P_0, \dots, P_{N-1} be a set of orthogonal polynomials in \mathcal{P}_N with $\langle P_i, P_j \rangle = 0$ for $i \neq j$ and the degree of P_n is n for each $0 \leq n \leq N-1$. Then for any $f \in \mathcal{H}_{\mu_t}$, the optimal approximation in $L_2(\mu_t)$ distance in \mathcal{P}_N is given by

$$\Pi(f) = \sum_{n=0}^{N-1} \langle f, P_n \rangle \frac{P_n}{\|P_n\|_{\mu_t}^2}, \quad (23)$$

where we define Π to be the projection operator. Now we turn to $\mathcal{L}_t(Z; G, X, \mu)$, viewing x_v as a function on $[0, t]$ for any v , we have:

$$\mathcal{L}_t(Z; G, X, \mu) = \int_0^t \sum_{v \in V} (x_v(s) - z_v(s))^2 d\mu_t(s) + \alpha \int_0^t Z(s)^\top L(s) Z(s) d\mu_t(s) \quad (24)$$

$$= \int_0^t \sum_{v \in V} (x_v(s) - \Pi(x_v)(s))^2 d\mu_t(s) \quad (25)$$

$$+ \int_0^t \sum_{v \in V} (\Pi(x_v)(s) - z_v(s))^2 d\mu_t(s) + \alpha \int_0^t Z(s)^\top L(s) Z(s) d\mu_t(s) \quad (26)$$

$$:= \int_0^t \sum_{v \in V} (x_v(s) - \Pi(x_v)(s))^2 d\mu_t(s) + \underline{\mathcal{L}}_t(Z; G, X, \mu) \quad (27)$$

The preceding display suggest that the minimizer of $\mathcal{L}_t(Z; G, X, \mu)$ is the same as the minimizer of $\underline{\mathcal{L}}_t(Z; G, X, \mu)$. It thus suffices to analyze $\underline{\mathcal{L}}_t(Z; G, X, \mu)$ which is easier to work with since $\Pi(x_v) \in \mathcal{P}_N, \forall v \in V$ and the solution is a direct application of Laplacian regularization with respect to the integrand at any $s \in [0, t]$, yielding:

$$\text{GPROJ}_t(G, X)(s) = (1 + \alpha L(s))^{-1} \Pi(X)(s), \quad (28)$$

Now let the coefficient matrix $Q \in \mathbb{R}^{N_V \times N}$ be defined as $Q_{v,n} = \langle x_v, P_n \rangle, \forall v \in V, n \in [N]$, we obtain the GHIPPO operator as:

$$\text{GHIPPO}(G, X)(s) := U(s) = (1 + \alpha L(s))^{-1} Q(s) \quad (29)$$

Next we take derivatives to the coefficients. Note that $L(t)$ is discontinuous and we can only apply derivative on intervals where $L(t)$ remains same. First note that if we choose μ_t to be the scaled Legendre measure (LegS) with $\mu_t = \frac{1}{t} \mathbb{I}_{[0,t]}$, and P_n as basic Legendre polynomials [11, Appendix B.1.1], then we have the HiPPO property:

$$\frac{dQ(t)}{dt} = Q(t)A^\top + X(t)B^\top \quad (30)$$

where $A \in \mathbb{R}^{N \times N}, B \in \mathbb{R}^{N \times 1}$ with

$$A_{nk} = - \begin{cases} \sqrt{(2n+1)(2k+1)} & \text{if } n > k, \\ n+1 & \text{if } n = k, \\ 0 & \text{if } n < k, \end{cases} \quad B_n = \sqrt{2n+1} \quad (31)$$

Fix some $1 \leq m \leq M$ and for $t \in [t_{m-1}, t_m)$ we have:

$$\frac{dU(t)}{dt} = \left((1 + \alpha L(t))^{-1} \right) \frac{dQ(t)}{dt} \quad (32)$$

$$= (1 + \alpha L(t))^{-1} (Q(t)A^\top + X(t)B^\top) \quad (33)$$

$$= U(t)A^\top + (1 + \alpha L(t))^{-1} X(t)B^\top. \quad (34)$$

which finishes the proof. \square

C.2 Proof of theorem 2

Proof of theorem 2. For ease of presentation, we operate on the node level instead of graph level. Recall the unobserved dynamics:

$$G_{l-1} = G_{l,0} \xrightarrow{\mathcal{E}_{l,1}} G_{l,1} \xrightarrow{\mathcal{E}_{l,2}} G_{l,2} \longrightarrow \cdots \longrightarrow G_{l,M_l-1} \xrightarrow{\mathcal{E}_{l,M_l}} G_{l,M_l} = G_l \quad (35)$$

Following the assumptions, we can intuitively write the update process as follows:

$$U_{l-1} = U_{l,0} \xrightarrow{G_{l,1}, X_{l,1}} U_{l,1} \xrightarrow{G_{l,2}, X_{l,2}} U_{l,2} \longrightarrow \cdots \longrightarrow U_{l,M_l-1} \xrightarrow{G_{l,M_l}, X_{l,M_l}} U_{l,M_l} = U_l \quad (36)$$

For each $0 \leq i \leq M_l$, let $D_i := (I + \alpha L_{l,i})^{-1} X_{l,i} B^\top$. Let $d_{v,i}$ be the v -th row of D_i and $u_{v,i}$ be the v -th row of $U_{l,i}$. We first write the ZOH update corresponding to each step in (36) for every $v \in V$:

$$u_{v,i} = \begin{cases} e^{(t_i - t_{i-1})A} u_{v,i-1} + A^{-1} (e^{(t_i - t_{i-1})A} - I) d_{v,i}, & \text{for } 1 \leq i \leq M_l \\ u_{v,l} & \text{for } i = 0 \end{cases} \quad (37)$$

Next we do the recursion from the rightmost to the leftmost according to (8):

$$\begin{aligned} u_{v,l} &= e^{(\tau_l - t_{M_l})A} u_{v,M_l} + A^{-1} (e^{(\tau_l - t_{M_l})A} - I) d_{v,M_l} \\ &= e^{(\tau_l - t_{M_l})A} \left(e^{(t_{M_l} - t_{M_l-1})A} u_{v,M_l-1} + A^{-1} (e^{(t_{M_l} - t_{M_l-1})A} - I) u_{v,M_l-1} \right) \\ &\quad + A^{-1} (e^{(\tau_l - t_{M_l})A} - I) u_{v,M_l} \\ &\dots \\ &= e^{(\tau_l - \tau_{l-1})A} u_{v,l-1} + \Upsilon \end{aligned} \quad (38)$$

where we define

$$\Upsilon = A^{-1} (e^{(\tau_l - t_{M_l})A} - I) u_{v,M_l} + \sum_{i=1}^{M_l} e^{(\tau_l - t_i)A} A^{-1} (e^{(t_i - t_{i-1})A} - I) u_{v,i-1} \quad (39)$$

in the above display we define $t_0 = \tau_{l-1}$. Note that A^{-1} and $e^{A\beta}$ are simultaneously diagonalizable for any β , therefore the matrix multiplication commutes and we further write

$$\Upsilon = A^{-1} (e^{(\tau_l - t_{M_l})A} - I) u_{v,M_l} + \sum_{i=1}^{M_l} A^{-1} (e^{(\tau_l - t_{i-1})A} - e^{(\tau_l - t_i)A}) u_{v,i-1} \quad (40)$$

With some abuse of notation now we let $A \in \mathbb{R}^N$ denote the diagonal vector of the matrix. We provide the following construction:

$$\lambda_i = \begin{cases} \frac{e^{(\tau_l - t_{M_l})A} - I}{e^{(\tau_l - \tau_{l-1})A} - I} & i = M_l \\ \frac{e^{(\tau_l - t_{i-1})A} - e^{(\tau_l - t_i)A}}{e^{(\tau_l - \tau_{l-1})A} - I} & 0 \leq i \leq M_l - 1 \end{cases}. \quad (41)$$

Here note that $\lambda_i \in \mathbb{R}^N$. It is straightforward to verify that:

$$\Upsilon = A^{-1} (e^{(\tau_l - \tau_{l-1})A} - I) \sum_{i=0}^{M_l} \lambda_i \odot u_{v,i} \quad (42)$$

where $\{\lambda_i\}_{0 \leq i \leq M_l}$ are non-negative N -dimensional vectors satisfying $\sum_{i=0}^{M_l} \lambda_i = \mathbf{1}_N$, with $\mathbf{1}_N$ denoting the all-one vector of dimension N . As the values of λ_i are *independent* of v , the proof finishes by combining (38), (42) and write the above conclusion in matrix form via setting $\Lambda_i = \text{diag}(\lambda_i)$, $0 \leq i \leq M_l$ \square

D Algorithm descriptions

D.1 The designs of mixing mechanism MIX

We consider two types of mixing mechanisms: convolution (CONV1D) and Scaled interpolation (INTERP) which we describe below:

CONV1D This is the usual convolution operation along the sequence dimension using *shared parameters*. We use a kernel size of 2 so that only consecutive representations are mixed.

INTERP This is an input dependent weighted average strategy followed by an input-dependent scaling, implemented as

$$\text{MIX}(Z_1, Z_2) = \rho(Z_1, Z_2) \odot (\xi(Z_1, Z_2) \odot Z_1 + (1 - \xi(Z_1, Z_2)) \odot Z_2), \quad (43)$$

where $Z_1, Z_2 \in \mathbb{R}^{N_V \times d}$ are node representation matrices corresponding to consecutive snapshots. ρ and ξ are scale and weight functions that maps two inputs into positive real numbers of identical shape with Z_1 or Z_2 , defined by

$$\rho(Z_1, Z_2) = \text{softplus}(W_\rho[Z_1 \| Z_2] + b_\rho), \quad \xi(Z_1, Z_2) = \text{sigmoid}(W_\xi[Z_1 \| Z_2] + b_\xi) \quad (44)$$

where $W_\rho, W_\xi \in \mathbb{R}^{2d \times d}$ and $b_\rho, b_\xi \in \mathbb{R}^d$ are learnable parameters therein.

D.2 Details of GRAPHSSM

In this section, we elucidate on the methodology of GRAPHSSM through three specific instantiations. For clarity in our explanation, we employ certain notational conventions which might be somewhat different from the main text: the term V refers to the number of vertices in each graph snapshot G_l within a sequence of L graph snapshots $\{G_l\}_{1 \leq l \leq L}$ which we further denote as $G_{1:L}$, and D represents the dimensionality of node features. The symbol lin is used to represent a linear projection layer including a bias term, where the dimensions for input and output are typically clear from the context to ensure compatibility. The notation $X_{1:L}$ denotes the concatenation of L tensors of the same dimensions along their second axis. For operations on tensors of order higher than two, we use the `einsum` notation, as defined by the `einops` framework [36]. We present the algorithmic description of our design of SSM layers, namely GRAPHSSM-S4 (resp. GRAPHSSM-S5, GRAPHSSM-S6) in algorithm 1 (resp. algorithm 2, algorithm 3).⁵ Subsequently, we adopt the following neural

Algorithm 1 GRAPHSSM-S4 layer

Input: A sequence of graph (snapshots) $G_{1:L}$ with each of size V .

Node (hidden) feature inputs $X_{1:L} \in \mathbb{R}^{V \times L \times D}$.

A graph neural network GNN_θ parameterized by θ .

A mixing mechanism MIX_ϕ parameterized by ϕ .

State-space parameters $A \in \mathbb{R}^{D \times N}$, $B \in \mathbb{R}^{D \times N}$, $C \in \mathbb{R}^{D \times N}$.

A linear layer for adaptive time gaps lin_τ .

Output: $Y_{1:L} \in \mathbb{R}^{V \times L \times D}$

```

1: # Approximate diffusion via GNN
2: for  $t = 1$  to  $L$  do
3:    $Z_l = \text{GNN}_\theta(X_l, G_l)$ ;
4:    $H_l = Z_l$  if  $l = 1$  else  $\text{MIX}(Z_l, Z_{l-1})$ ;
5: end for
6: Initialize state  $U_0 = 0$ ; # SISO state of shape  $V \times D \times N$ 
7: for  $t = 1$  to  $L$  do
8:    $\Delta_l = \text{softplus}(\text{lin}_\tau(H_l))$ ;
9:    $\bar{A} = \exp(\text{einsum}(\Delta_l, A, "V, DN \rightarrow VDN"))$ ;
10:   $\bar{B} = \text{einsum}(\Delta_l, B, "V, DN \rightarrow VDN")$ ;
11:   $U_l = U_{l-1} \odot \bar{A} + \text{einsum}(\bar{B}, H_l, "VDN, VD \rightarrow VDN")$ ;
12:   $Y_l = \text{einsum}(U_l, C, "VDN, DN \rightarrow VD")$ ;
13: end for;
14: return  $Y_{1:L}$ ;
```

architecture composed of K blocks, with each block composed of one SSM layer followed by nonlinear activation and a residual connection:

$$H_{1:L}^{(k)} = \sigma \left(\text{SSMLAYER} \left(H_{1:L}^{(k-1)}, G_{1:L} \right) \right) + \text{lin} \left(H_{1:L}^{(k-1)} \right), 1 \leq k \leq K, \quad (45)$$

where $H_{1:L}^{(0)}$ are the node features $X_{1:L}$. The SSMLAYER in (45) may be chosen as any of {GRAPHSSM-S4, GRAPHSSM-S5, GRAPHSSM-S6}. In our implementation of GRAPHSSM-S6, we add an additional layer normalization as the last operation of each block.

⁵In these algorithmic descriptions, we illustrate using the **representation mixing** mechanism. The case for **feature mixing** is similarly defined.

Algorithm 2 GRAPHSSM-S5 layer

Input: A sequence of graph (snapshots) $G_{1:L}$ with each of size V .

Node (hidden) feature inputs $X_{1:L} \in \mathbb{R}^{V \times L \times D}$.

A graph neural network GNN_θ parameterized by θ .

A mixing mechanism MIX_ϕ parameterized by ϕ .

State-space parameters $A \in \mathbb{R}^{N \times 1}$, $B \in \mathbb{R}^{D \times N}$, $C \in \mathbb{R}^{N \times D}$.

A linear layer for adaptive time gaps lin_τ .

Output: $Y_{1:L} \in \mathbb{R}^{V \times L \times D}$

```
1: # Approximate diffusion via GNN
2: for  $t = 1$  to  $L$  do
3:    $Z_t = \text{GNN}_\theta(X_t, G_t)$ ;
4:    $H_t = Z_t$  if  $l = 1$  else  $\text{MIX}(Z_t, Z_{t-1})$ ;
5: end for
6: Initialize state  $U_0 = 0$ ; # MIMO state of shape  $V \times N$ 
7: for  $t = 1$  to  $L$  do
8:    $\Delta_t = \text{softplus}(\text{lin}_\tau(H_t))$ ;
9:    $\bar{A} = \exp(\Delta_t A^\top)$ ;
10:   $\bar{B} = \text{einsum}(\Delta_t, B, "V, DN \rightarrow VDN")$ ;
11:   $U_t = U_{t-1} \odot \bar{A} + \text{einsum}(\bar{B}, H_t, "VDN, VD \rightarrow VN")$ ;
12:   $Y_t = U_t C$ ;
13: end for;
14: return  $Y_{1:L}$ ;
```

Initialization strategy Recent developments in state space modeling have underscored the significance of initializing the state matrices A , B , and C , with the initialization of A frequently emerging as the most critical factor for the performance of the SSM [12]. Building upon the progress made in S4 [13] and S4D [28, 15], we evaluate three disparate initialization strategies for the matrix A . Note that since A is diagonal, we instead represent A as a N -dimensional vector:

$$\forall 1 \leq n \leq N : \quad A_n^{\text{S4D-Real}} = -(n+1), \quad A_n^{\text{S4D-Const}} \equiv \frac{1}{2}, \quad A_n^{\text{random}} = -e^\chi \quad (46)$$

S4D-Real(HiPPO) This is the diagonal part of the original HiPPO matrices (6).

S4D-Const(Constant) This is the real part of the eigenvalues corresponding to the S4N matrix as defined in [13], which equals $-\frac{1}{2}$.

Random This initialization is generated via a negative transform of a random number χ , where we generated using the Glorot initialization method.

Additionally, we initialize the B matrices using a constant of all-1 vector, and we initialize C randomly using Glorot.

D.3 Complexity and implementations

As detailed in Section 3.1 and the algorithmic outlines provided, the implementations of GRAPHSSM across all three variants can be stratified into two primary phases: a diffuse-and-mixing step, and a linear recurrence step. The diffuse-and-mixing stage facilitates straightforward parallelization through the employment of methods such as graph batching. The inherent linear characteristic of the recurrence operation permits the utilization of efficient computation strategies, notably the selective scan technique as introduced in [10]. This approach yields a FLOP complexity of $O(VLDN)$ per SSM layer with work-efficient parallelization, concurrently achieving IO efficiency. Furthermore, note that if we replace the adaptive time gap mechanism into a constant, i.e., we use $\Delta_t \equiv \frac{1}{L}$, $1 \leq l \leq L$ in line 8 of algorithm 1 and algorithm 2, the resulting linear system is time-invariant and we can use other computational accelerations like convolution [13, 7] and parallel scan [39].

Algorithm 3 GRAPHSSM-S6 layer

Input: A sequence of graph (snapshots) $G_{1:L}$ with each of size V .

Node (hidden) feature inputs $X_{1:L} \in \mathbb{R}^{V \times L \times D}$.

A graph neural network GNN_θ parameterized by θ .

Three graph neural networks for selective state spaces $\text{GNN}_{\theta_B}, \text{GNN}_{\theta_C}, \text{GNN}_\Delta$.

A mixing mechanism MIX_ϕ parameterized by ϕ .

State-space parameters $A \in \mathbb{R}^{D \times N}$.

Output: $Y_{1:L} \in \mathbb{R}^{V \times L \times D}$

```
1: # Approximate diffusion via GNN
2: for  $t = 1$  to  $L$  do
3:    $Z_t = \text{GNN}_\theta(X_t, G_t)$ ;
4:    $H_t = Z_t$  if  $l = 1$  else  $\text{MIX}(Z_t, Z_{t-1})$ ;
5: end for
6: Initialize state  $U_0 = 0$ ; # SISO state of shape  $V \times D \times N$ 
7: for  $t = 1$  to  $L$  do
8:    $\Delta_t = \text{softplus}(\text{GNN}_\Delta(X_t, G_t) + b)$ ;
9:    $\bar{A} = \exp(\text{einsum}(\Delta_t, A, "VD, DN \rightarrow VDN"))$ ;
10:   $\bar{B} = \text{einsum}(\Delta_t, \text{GNN}_{\theta_B}(X_t, G_t), "VD, VN \rightarrow VDN")$ ;
11:   $U_t = U_{t-1} \odot \bar{A} + \text{einsum}(\bar{B}, H_t, "VDN, VD \rightarrow VDN")$ ;
12:   $\bar{C} = \text{GNN}_{\theta_C}(X_t, G_t)$ ;
13:   $Y_t = \text{einsum}(U_t, \bar{C}, "VDN, DN \rightarrow VD")$ ;
14: end for;
15: return  $Y_{1:L}$ ;
```

E Discussions and limitations

In this section, we discuss the limitations of the GRAPHSSM framework and propose a few future research directions that might be of interest.

E.1 Extension to continuous-time temporal graphs

In this study, we concentrate on modeling discrete-time temporal graphs through the lens of discretizing continuously evolving systems. The continuous-time viewpoint holds promise for encapsulating the modeling of continuous-time temporal graphs (CTTGs), a domain of growing importance within the realm of contemporary graph modeling. This perspective hinges on the concept that temporal graphs are generated through a chronology of events, each marked by precise temporal occurrences. Nevertheless, the transition to modeling CTTGs introduces novel algorithmic complications, hindering the straightforward application of our proposed framework (GRAPHSSM), despite the applicability of the core principle of GHIPPO to CTTGs.

A notable challenge arises from the way structural alterations, instigated by any single event, precipitate shifts in the dynamics affecting an extensive subset of nodes—not limited to those directly involved in the event. Specifically, nodes within the same connected component as those affected by the event (referred to as 'infected' nodes) experience these dynamic shifts. Within the context of a large-scale system, this intricacy renders the update mechanism exceedingly complex. Consequently, there arises a necessity to employ approximation strategies and develop efficient streaming update tactics tailored to this extensive system. Addressing these challenges through innovative solutions represents an intriguing direction for future research.

E.2 Going beyond piecewise dynamics

The distinguishing algorithmic feature of GHIPPO compared to the conventional HIPPO framework lies in the piecewise nature of the dynamical system it generates. This characteristic leads to the challenge of dealing with unobserved dynamics, a factor that motivated the development of our MIX module. However, it's important to acknowledge that the mixing module serves as an approximation of the actual underlying dynamics, thus representing a limitation within the framework. This

acknowledgment raises an intriguing question: might there exist alternative problem formulations capable of yielding a smoother dynamical system, one devoid of discontinuities? One potential pathway could involve adopting smoother versions of the Laplacian or revising the approximation objective specified in (3) towards one that fosters a smooth solution. Such a solution would promote consistency in the dynamics across the complete temporal interval. Implementing these innovations would, however, necessitate the incorporation of more sophisticated technical assumptions and theoretical tools which we left to future explorations.

F Experimental setup

Table 6: Dataset Statistics.

	DBLP-3	Brain	Reddit	DBLP-10	arXiv	Tmall
#Nodes	4,257	5,000	8,291	28,085	169,343	577,314
#Edges	23,540	1,955,488	264,050	236,894	2,315,598	4,807,545
#Features	100	20	20	128	128	128
#Classes	3	10	4	10	40	5
#Time Steps	10	12	10	27	35	186
Category	Citation	Biology	Society	Citation	Citation	E-commerce
TC_{structure}	0.139	0.024	0.030	0.823	0.580	0.811
TC_{feature}	0.468	0.070	0.556	0.823	1.000	0.712

Temporal continuity. As illustrated in Figure 2, our work has highlighted the problem of unobserved graph mutations in learning from discrete-time temporal graphs. The issue of unobserved graph mutations greatly hampers the temporal continuity of such graphs, presenting a significant challenge for learning if not properly addressed. To quantitatively measure the temporal continuity of a temporal graph, we calculate the average proximity between consecutive graph snapshots in the graph sequence. Specifically, we utilize Jaccard distance and Cosine similarity to measure the temporal continuity in terms of graph structure and node features, respectively:

$$\begin{aligned}
\text{TC}_{\text{structure}} &= \frac{1}{L-1} \sum_l^{L-1} \frac{\mathcal{E}_l \cap \mathcal{E}_{l+1}}{\mathcal{E}_l \cup \mathcal{E}_{l+1}}, \\
\text{TC}_{\text{feature}} &= \frac{1}{L-1} \sum_l^{L-1} \text{Sim}(X_l, X_{l+1}), \\
\text{where } \text{Sim}(X_l, X_{l+1}) &= \frac{1}{N_V} \sum_{v \in V} \frac{\langle x_{l,v}, x_{l+1,v} \rangle}{\|x_{l,v}\| \|x_{l+1,v}\|}.
\end{aligned} \tag{47}$$

Datasets. We focus on the node classification task in discrete-time temporal graphs, which is a straightforward extension of static graphs. The experiments are conducted on six temporal graph benchmarks with different scales and time snapshots, including DBLP-3 [45], Brain [45], Reddit [45], DBLP-10 [24], arXiv [19], and Tmall [24]. Dataset statistics are summarized in Table 6 including the corresponding temporal continuity. The graph datasets are collected from real-world networks belonging to different domains. It should be noted that in the arXiv dataset, the time information is associated with the nodes rather than the edges. As a result, we split the snapshots of arXiv based on the occurrence of nodes. Each snapshot graph in the dataset shares the same attribute information but not the topology. Therefore, $\text{TC}_{\text{feature}} = 1.000$ for arXiv in our experiments.

Baselines. We compare GRAPHSSM with the following baselines: (i) static graph embedding methods: DeepWalk [35], Node2Vec [9]; (ii) temporal graph embedding methods: HTNE, M²DNE, and DynamicTriad [48]; (iii) discrete-time temporal graph neural networks: MPNN [31], STAR [45], tNodeEmbed [38], EvolveGCN [33], SpikeNet [24], and ROLAND [46]. For baselines that are originally designed for static graphs, we accumulate historical information (edges) in the graph snapshot sequence and represent the static graph structure at the last time point. All baselines are carefully tuned to achieve their best results based on the code officially provided by the authors.

Implementation details. GRAPHSSM is built on the success of SSMs, where in this work we have derived variants of GRAPHSSM-S4, GRAPHSSM-S5, and GRAPHSSM-S6, under different SSM settings. Our experiments are mainly conducted on the S4 architecture. we employ feature mixing for DBLP-10 and representation mixing for other datasets. The graph convolution networks used to learn the graph structure are SAGE [16] for all datasets, except for arXiv, where GCN [22] is used. We implement our models as well as baselines with PyTorch [34] and PyTorch Geometric [5], which are open-source software released under BSD-style⁶ and MIT⁷ license, respectively. All datasets used throughout experiments are publicly available. All experiments are conducted on an NVIDIA RTX 3090 Ti GPU with 24 GB memory. Code will be made available at <https://github.com/EdisonLeeeee/GraphSSM>.

Evaluation protocol. We adopt the conventional *transductive* learning setting, where the graph structure of all snapshots is visible during both training and inference stages. This is analogous to the standard node classification task, but with the additional incorporation of time information to facilitate the learning. We follow the experimental settings of previous works [24], where 80% of the nodes are randomly selected as the training set, and the remaining nodes are used as the test set. Note that stratified sampling is used to ensure that the class distribution remains the same across splits. We use Micro-F1 and Macro-F1 to evaluate the node classification performance. We report the average performance with standard deviation across 5 runs for each method.

⁶<https://github.com/pytorch/pytorch/blob/master/LICENSE>

⁷https://github.com/pyg-team/pytorch_geometric/blob/master/LICENSE